Technical Notes

TECHNICAL NOTES are short manuscripts describing new developments or important results of a preliminary nature. These Notes cannot exceed 6 manuscript pages and 3 figures; a page of text may be substituted for a figure and vice versa. After informal review by the editors, they may be published within a few months of the date of receipt. Style requirements are the same as for regular contributions (see inside back cover).

AIAA 82-4146

Closed-Form Solutions of Supersonic Wing-Body Interference

Narendra R. Vira* and Dah-Nien Fan†
Howard University, Washington, D.C.

Nomenclature

A_W = wing reference area, $(d/2)C_r(1+\lambda)(s/r-1)$
Æ = wing-alone aspect ratio
B = $m\beta$
$(C_{L\alpha})_W$ = lift curve slope for wing alone
C_r = wing root chord
C_t = wing tip chord
D = $\beta d/C_r$
d = body diameter
$K_{B(W)}$ = interference factor for a body in the presence of a wing
$\bar{K}_{B(W)}$ = $K_{B(W)}(1+\lambda)\ (s/r-1)\beta(C_{L\alpha})_W$
L_W = lift of wing alone
$L_{B(W)}$ = lift transmitted on the body due to a wing panel
ℓ = length of afterbody
M_∞ = freestream Mach number
m = cotangent of leading-edge sweep angle
P = $\ell/\beta d$
q_∞ = freestream dynamic pressure
R = $P+1/D$
r = body radius
s = exposed wing semispan measured from root chord
α = angle of attack
β = $\sqrt{M_\infty^2-1}$
ξ = coordinate along longitudinal axis
η = coordinate along spanwise direction
μ = $\tan^{-1}(\beta)$
λ = wing taper ratio, C_t/C_r

Introduction

RECENTLY, Vukelich and Williams[1] calculated numerically the effects of finite afterbodies on the interference factor $K_{B(W)}$ for a body in the presence of a wing at supersonic speeds following the method used by Pitts et al.[2] The present Note shows that $K_{B(W)}$ for partial or finite afterbodies can be expressed in closed form just as those for no and full afterbodies[2] by explicitly evaluating the double integrals involved. Furthermore, this Note shows that, by a simple transformation, the zero-afterbody results become applicable to situations where the base of the body is forward of the trailing edge of the exposed root chord—resembling a "negative" afterbody.

Received July 6, 1981; revision received Oct. 9, 1981.

*Senior Graduate Research Assistant, Dept. of Mechanical Engineering. Student Member AIAA.
†Professor, Dept. of Mechanical Engineering. Member AIAA.

Analysis

The interference factor for a body in the presence of a wing is defined as[2]

$$K_{B(W)} \equiv \frac{2L_{B(W)}}{L_W} = \frac{2L_{B(W)}}{(C_{L\alpha})_W \alpha A_W q_\infty} \tag{1}$$

where $L_{B(W)}$ is given by

$$L_{B(W)} = \frac{8q_\infty \alpha B^{3/2}}{\pi\beta(1+B)}\left[\int_{\eta_1}^{\eta_2} d\eta \int_{\xi_1}^{\xi_2}\left(\frac{\xi/\beta-\eta}{m\xi+\eta}\right)^{1/2} d\xi + \int_{\eta_3}^{\eta_4} d\eta \int_{\xi_3}^{\xi_4}\left(\frac{\xi/\beta-\eta}{m\xi+\eta}\right)^{1/2} d\xi\right] \tag{2}$$

$$L_{B(W)} = \frac{4q_\infty \alpha m}{\pi(B^2-1)^{1/2}}\left[\int_{\eta_1}^{\eta_2} d\eta \int_{\xi_1}^{\xi_2}\cos^{-1}\left(\frac{\xi/\beta+m\beta\eta}{\eta+m\xi}\right) d\xi + \int_{\eta_3}^{\eta_4} d\eta \int_{\xi_3}^{\xi_4}\cos^{-1}\left(\frac{\xi/\beta+m\beta\eta}{\eta+m\xi}\right) d\xi\right] \tag{3}$$

for subsonic and supersonic leading edges, respectively, provided the condition Æ$(1+\lambda)(1+B^{-1})\geq 4$ and other assumptions inherent in the formulation of Ref. 2 are satisfied. The domains of integration are shown as shaded areas in Fig. 1 depending upon the value of R. In the (ξ,η) coordinate system the limits of integrations are thus those shown in Fig. 1. It should be noted that the planar models

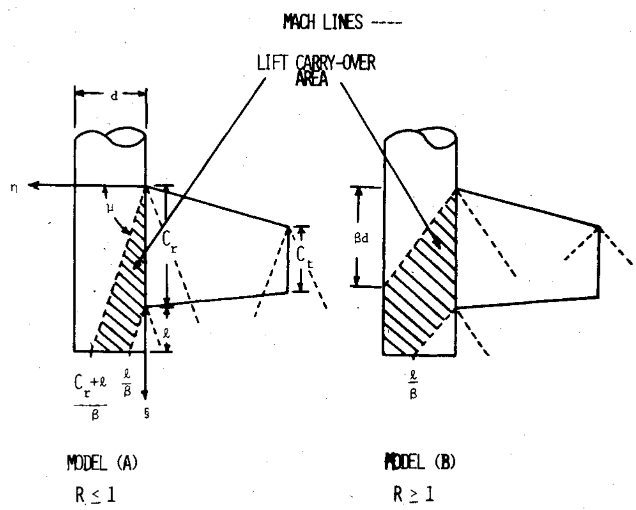

LIMITS OF INTEGRATION

$\xi_1 = \beta\eta = \xi_3$ $\qquad \eta_1 = 0$

$\xi_2 = C_r + \beta\eta$ $\qquad \eta_2 = \frac{\ell}{\beta} = \eta_3$

$\xi_4 = C_r + \ell$ $\qquad \eta_4 = \begin{cases}(C_r+\ell)/\beta, & R\leq 1\\ d, & R\geq 1\end{cases}$

Fig. 1 Lift carryover planar models for determination of $\bar{K}_{B(W)}$ at supersonic speeds with Æ$(1+\lambda)(1+B^{-1})\geq 4$.

shown in Fig. 1 contain the cases of no afterbody and full afterbody as special ones (see later subsection on special cases).

The integrals in $L_{B(W)}$ can be evaluated in closed form after some lengthy manipulations, and the respective interference factors are determined. Some details of the integration steps were documented in Ref. 3.

Subsonic Leading Edge ($B<1$)

It can be shown that the interference factors for models A and B in Fig. 1 are, respectively, in the case of subsonic leading edge,

$$\bar{K}_{B(W)}(R\leq 1)$$

$$=\frac{16B^{1/2}D}{\pi(B+1)}\left\{\frac{B^{3/2}}{D^2(1+B)}\left[\left(\frac{B+(1+B)PD}{B}\right)^{1/2}-2\right]\right.$$

$$\left.-\left(\frac{B}{1+B}\right)\frac{1}{\sqrt{D}}(BR+P)^{3/2}+B(1+B)R^2\tan^{-1}\left(\frac{1/D}{BR+P}\right)^{1/2}\right\} \tag{4}$$

$$\bar{K}_{B(W)}(R\geq 1)=\bar{K}_{B(W)}(R\leq 1)+\frac{16B^{1/2}D}{\pi(B+1)}\left\{(BR+1)\right.$$

$$\times\sqrt{(R-1)(BR+1)}-\frac{(B+1)}{\sqrt{B}}\tanh^{-1}\left(\frac{BR-B}{BR+1}\right)^{1/2}$$

$$\left.-B(1+B)R^2\tan^{-1}\left(\frac{R-1}{BR+1}\right)^{1/2}\right\} \tag{5}$$

Supersonic Leading Edge ($B>1$)

In the case of a supersonic leading edge, it can be similarly shown that the interference factors for models A and B are given by, respectively,

$$\bar{K}_{B(W)}(R\leq 1)=\frac{8D}{\pi(B^2-1)^{1/2}}\left\{\left(\frac{-B}{1+B}\right)(BR+P)^2\right.$$

$$\times\cos^{-1}\left(\frac{R+BP}{BR+P}\right)+\frac{B}{D^2}\frac{(B^2-1)^{1/2}}{(1+B)}[\sqrt{1+2PD}-1]$$

$$\left.-\frac{B^2}{D^2(1+B)}\cos^{-1}\frac{1}{B}+BR^2(B^2-1)^{1/2}\cos^{-1}\frac{P}{R}\right\} \tag{6}$$

$$\bar{K}_{B(W)}(R\geq 1)=\bar{K}_{B(W)}(R\leq 1)+\frac{8D}{\pi(B^2-1)^{1/2}}$$

$$\times\left\{(BR+1)^2\cos^{-1}\left(\frac{R+B}{BR+1}\right)-(B^2-1)^{1/2}\cosh^{-1}(R)\right.$$

$$\left.+BR^2(B^2-1)^{1/2}\left[\sin^{-1}\frac{1}{R}-\frac{\pi}{2}\right]\right\} \tag{7}$$

The expressions $R\leq 1$ and $R\geq 1$ in parentheses immediately after $\bar{K}_{B(W)}$ in Eqs. (4-7) are introduced to differentiate the cases of $R\leq 1$ and $R\geq 1$. The interference factor $\bar{K}_{B(W)}$ given by Eqs. (4-7) is a function of three independent parameters B, D, and P. Note that R depends on P and D. These parameters have been nondimensionalized in the same manner as was done in Ref. 2. Numerical computations using the closed-form formulas of Eqs. (4-7) are in agreement with the limited numerical-integration results given by Vukelich and Williams (Figs. 3 and 4 in Ref. 1).

Special Cases

No Afterbody ($P=0$)

Vanishing P corresponds to the case of no afterbody. For $P=0$ and $D\leq 1$, Eqs. (5) and (7) reduce to Eqs. (30) and (31) of Ref. 2 in full agreement. For $P=0$ and $D\geq 1$, Eqs. (4) and (6) reduce to Eqs. (5.3.8) and (5.3.10) of Ref. 3, again in full agreement. It should be mentioned that Ref. 2 gives only charts of interference factors for $P=0$ and $D\geq 1$.

Full/Infinite Afterbody ($P\geq 1$)

It can be easily shown that $R\geq 1$ when $P=1$. Thus Eqs. (5) and (7) after substituting $P=1$ lead to the same expressions for $\bar{K}_{B(W)}$ as in Ref. 2, Eqs. (24) and (26). It is clear that $\bar{K}_{B(W)}(P>1)=\bar{K}_{B(W)}(P=1)$. Equations (4) and (6), being valid only for $R\leq 1$, should be disregarded for the case of full/infinite afterbody.

"Negative" Afterbody

By "negative" afterbody we mean that the base of the body is forward of the trailing edge of the exposed root chord and the parameter P is negative. The interference factor $\bar{K}_{B(W)}$ for negative afterbody can be obtained by first letting $P=0$ in Eqs. (4-7) and then replacing D in the resulting expressions by the transformation

$$D=D_n/(1+P_nD_n)=1/R_n \tag{8}$$

Note that the subscript n stands for negative afterbody and will be dropped hereafter. Thus, the interference factors for models A and B when $-1/D\leq P\leq 0$ are, respectively, in the case of subsonic leading edge

$$\bar{K}_{B(W)}(0\leq R\leq 1)=\frac{16BR}{\pi(1+B)}\left[B^{1/2}(1+B)\tan^{-1}\left(\frac{1}{B}\right)^{1/2}-B\right] \tag{9}$$

$$\bar{K}_{B(W)}(R\geq 1)=\bar{K}_{B(W)}(0\leq R\leq 1)$$

$$+\frac{16B^{1/2}}{\pi(B+1)R}\left[(BR+1)\sqrt{(R-1)(BR+1)}\right.$$

$$\left.-\frac{B+1}{B^{1/2}}\tanh^{-1}\left(\frac{BR-B}{BR+1}\right)^{1/2}-B(1+B)R^2\tan^{-1}\left(\frac{R-1}{BR+1}\right)^{1/2}\right] \tag{10}$$

Similarly, in the case of supersonic leading edge they are, respectively,

$$\bar{K}_{B(W)}(0\leq R\leq 1)=\frac{8BR}{\pi(B^2-1)^{1/2}}\left[(B^2-1)^{1/2}\frac{\pi}{2}-B\cos^{-1}\frac{1}{B}\right] \tag{11}$$

$$\bar{K}_{B(W)}(R\geq 1)=\bar{K}_{B(W)}(0\leq R\leq 1)+\frac{8}{\pi(B^2-1)^{1/2}R}$$

$$\times\left[(BR+1)^2\cos^{-1}\left(\frac{R+B}{BR+1}\right)-(B^2-1)^{1/2}\cosh^{-1}R\right.$$

$$\left.+BR^2(B^2-1)^{1/2}\left(\sin^{-1}\frac{1}{R}-\frac{\pi}{2}\right)\right] \tag{12}$$

Mathematically $\bar{K}_{B(W)}(R\leq 0)=0$.

In Fig. 2 a graphical procedure for obtaining $\bar{K}_{B(W)}$ for negative afterbodies is presented. The interference factor for zero afterbody of Ref. 2 is reproduced in the lower-left portion of Fig. 2, and the upper-right portion gives the transformation [Eq. (8)] with the product $P_nD_n=\ell/C_r$ as a parameter. With the effective D value determined from an

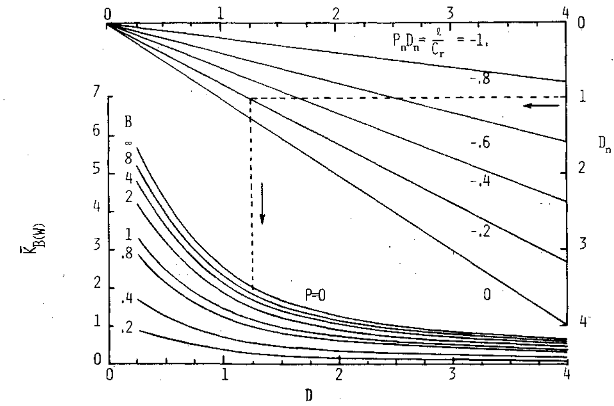

Fig. 2 Design chart to determine $\bar{K}_{B(W)}$ for negative afterbody from $\bar{K}_{B(W)}$ for no afterbody.

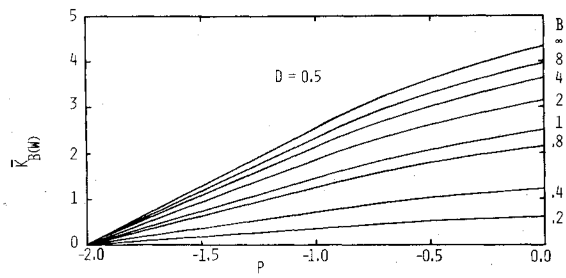

Fig. 3 $\bar{K}_{B(W)}$ for negative afterbody as a function of afterbody length. (If you relabel the abscissa as $R = P + 2$, this figure is applicable for all P and D with $0 \leq R \leq 2$.)

upper-half straight line from specified values of D_n and ℓ/C_r, $\bar{K}_{B(W)}$ then can be looked up from a lower-half curve for a given B. For example, Fig. 2 yields $\bar{K}_{B(W)} \approx 2$ and $D \approx 1.25$ for $D_n = 1$, $\ell/C_r = -0.2$, and $B \rightarrow \infty$.

Variation of $\bar{K}_{B(W)}$ with respect to afterbody length is illustrated in Fig. 3 for the full range of B values. Note that for a fixed B the dependence of $\bar{K}_{B(W)}$ on R is linear if R is less than or equal to unity.

Conclusion

Closed-form formulas have been presented for the interference factors $\bar{K}_{B(W)}$ for a body in the presence of a wing at supersonic speeds when a finite afterbody is introduced. In addition, formulas for $\bar{K}_{B(W)}$'s have been obtained for situations when the base of the body is forward of the trailing edge of the exposed root chord (negative afterbody). These formulas are valid subject to the restrictions inherent in the formulation of Ref. 2.

Remarks

Similar to $\bar{K}_{B(W)}$, the body longitudinal center-of-pressure location can be determined in closed form. This work is currently in progress and will be reported later.

Acknowledgments

Support of this work by NASA Contract NAS5-24242 to Howard University is hereby gratefully acknowledged. The authors wish to express their thanks to the technical officer of the contract, Mr. James S. Barrowman, Code 742, at the NASA Goddard Space Flight Center in Greenbelt, Md.

References

[1] Vukelich, S. R. and Williams, J.E. Jr., "Wing-Body Carryover at Supersonic Speeds with Finite Afterbodies," *AIAA Journal*, Vol. 19, May 1981, pp. 661-664.

[2] Pitts, W. C., Nielsen, J. N., and Kaattari, G. E., "Lift and Center of Pressure of Wing-Body-Tail Combinations at Subsonic, Transonic, and Supersonic Speeds," NACA 1307, 1959.

[3] Fan, D. N. and Vira, N. R., "Aerodynamics of Sounding Rockets," Dept. of Mechanical Engineering, Howard University, Washington, D.C., Annual Report to the NASA Goddard Space Flight Center, NASA Contract NAS5-24242, Oct. 1980.

AIAA 82-4147

Calculation of Unsteady Transonic Flows with Shocks by Field Panel Methods

Michael H. L. Hounjet*
National Aerospace Laboratory NLR
Amsterdam, the Netherlands

Introduction

To date the various successful finite difference methods (FDM)[1,2] to investigate unsteady inviscid transonic flow have almost overshadowed other methods. Although the computation times of the versions for two-dimensional flow are reasonable, the prospects for three-dimensional flow are unattractive. At NLR, therefore, activities were begun a few years ago to develop competitive integral equation methods (IEM). For steady flow this work has resulted in the NLR field panel method (FPM),[3] and improvements are being attempted.[4] The purpose of this Note is to indicate the status of developments for unsteady flow.

IEM Formulation

First the basic equations for an unsteady IEM are briefly described. The boundary-value problem that governs the unsteady "time-linearized" inviscid transonic potential flow past a thin two-dimensional wing at a small angle of attack is shown in Fig. 1. There, M is the freestream Mach number; k the reduced frequency, $k = \omega c/2U$, where c denotes the chord; and U the undisturbed flow speed. $\Phi^{(0)}$ and $\Phi^{(1)}$ denote the mean steady and the first harmonic component of the perturbation velocity potential, and H the amplitude of oscillation of the mean wing surface. γ^* is defined[1] by: $\gamma^* = 2 - (2-\gamma)M^2$. The variables are all made dimensionless with c and U. The pressure coefficient $C_p^{(1)}$ is made dimensionless with the dynamic pressure. An exact solution of this boundary-value problem will show a jump in $\Phi^{(1)}$ across the steady-shock location which is proportional to the integrated pressure coefficient inside the shock trajectory.[5] A solution of the boundary-value problem can be expressed by:

$$\Phi^{(1)}(x,y) = \int_0^\infty \Delta\Phi^{(1)}(u) \frac{\partial}{\partial y} E(x-u,y)\,du + \int_{-\infty}^{\infty}\int_{-\infty}^{\infty} m(u,v) E(x-u,y-v)\,du\,dv \qquad (1)$$

where $E(x,y)$ satisfies the radiation condition and

$$(1-M^2)E_{xx} + E_{yy} - 2ikM^2E_x + k^2M^2E = \delta(x)\delta(y) \qquad (2)$$

Received July 6, 1981; revision received Nov. 2, 1981.

*Research Engineer, Dept. of Aeroelasticity.